

See discussions, stats, and author profiles for this publication at: <https://www.researchgate.net/publication/6015077>

Ab Initio Investigation on the Second-Order Nonlinear Optical Responses in Keto–Enol Equilibria of Salicylideneanilines

ARTICLE *in* THE JOURNAL OF PHYSICAL CHEMISTRY A · NOVEMBER 2007

Impact Factor: 2.69 · DOI: 10.1021/jp074567e · Source: PubMed

CITATIONS

25

READS

50

5 AUTHORS, INCLUDING:



Maxime Guillaume

Solvay

35 PUBLICATIONS 731 CITATIONS

[SEE PROFILE](#)



Nadezhda Markova

Bulgarian Academy of Sciences

20 PUBLICATIONS 184 CITATIONS

[SEE PROFILE](#)



Venelin Enchev

Bulgarian Academy of Sciences

103 PUBLICATIONS 808 CITATIONS

[SEE PROFILE](#)



Frédéric Castet

Université of Bordeaux

90 PUBLICATIONS 1,694 CITATIONS

[SEE PROFILE](#)

Ab Initio Investigation on the Second-Order Nonlinear Optical Responses in Keto–Enol Equilibria of Salicylideneanilines

Maxime Guillaume and Benoît Champagne*

Laboratoire de Chimie Théorique Appliquée, Facultés Universitaires Notre-Dame de la Paix (FUNDP),
rue de Bruxelles 61, B-5000 Namur, Belgium

Nadezhda Markova and Venelin Enchev

Institute of Organic Chemistry, Bulgarian Academy of Sciences, 1113 Sofia, Bulgaria

Frédéric Castet

Institut des Sciences Moléculaires, UMR 5255 CNRS, Université de Bordeaux I,
Cours de la Libération, 351, F-33405 Talence Cedex, France

Received: June 13, 2007; In Final Form: July 5, 2007

The keto–enol (K–E) tautomerization equilibrium, more precisely, the keto-amine/enol-imine equilibrium, has been investigated for a series of substituted salicylideneanilines in view of designing compounds with a contrast of second-order nonlinear optical properties. Substituting the salicylidene ring by an acceptor group or the other ring by a donor prevents the K form from being stable, whereas in the other cases, the K form can easily be converted to the E form due to the small activation barrier, figuring out in most cases that the K form is metastable. For a representative set of donor/acceptor substituents, the E and K forms present a sufficiently large contrast of β to allow its detection by using electric-field-induced second harmonic generation or hyper-Rayleigh scattering. The largest β values are mainly associated with species bearing a donor in the para position of the salicylidene ring and an acceptor on the other ring whereas the largest β values are generally found for the E form.

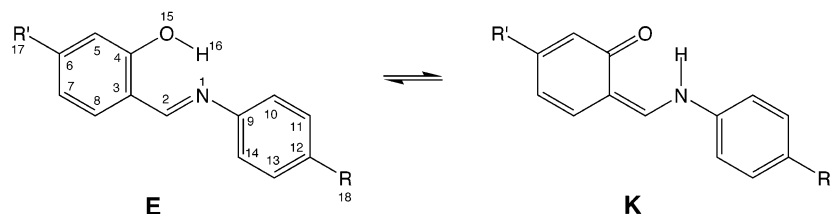
1. Introduction

Schiff bases, derivatives of aromatic *o*-hydroxyaldehydes, are a class of compounds which have received attention owing to their interesting linear and nonlinear optical properties, biological activity, and technological applications.^{1–5} In salicylideneanilines and related Schiff bases, generally called anils, an intramolecular proton-transfer reaction between the enol-imine (E) and keto-amine (enaminone) (K) forms can occur both in solution and in the crystalline state (Figure 1a). This reaction can be triggered either by light or by heat and can even be encountered in biological media.⁶ The associated photo- and thermochromisms make salicylideneaniline-like compounds intelligent materials, which can be used as molecular switches and memories.⁷ Many references mention that thermo- and photochromism are mutually exclusive in anil crystals, but a recent paper presents a compound exhibiting both properties.⁸

In Schiff bases with intramolecular H-bonds, such as derivatives of aromatic *o*-hydroxyaldehydes condensed with primary amines (Figure 1), the E form is usually the most stable one. Some exceptions have however been observed,⁹ including for Schiff bases derived from the condensation of 2-hydroxynaphthalene-1-carbaldehyde with primary amines.^{10–11} Usually, the E form is colorless or slightly yellow with an absorption band in the near UV, whereas the K form is red and exhibits an additional absorption band for wavelength larger than 400 nm. The $E \rightleftharpoons K$ equilibrium is indeed influenced by the nature of the substituents on the salicylidene moiety. For instance, the

presence of a second vicinal hydroxyl group on the salicylidene ring (position 5 on Figure 1a), which participates in intermolecular H-bonding, results in the coexistence of the K form in significant amounts in the crystalline state.¹² Besides the modifications of the thermodynamical aspects (energies of reaction and energies of activation), varying the substituents has an impact on the other molecular properties: absorption and emission spectra, vibrational signatures, as well as linear and nonlinear optical (NLO) properties. Following the investigations by several groups,^{13–16} this paper addresses the NLO properties of substituted salicylideneanilines and in particular their variations upon switching between the K and E forms. For instance, *N*-salicylidene-2-chloro-4-nitroaniline has been shown to present a first hyperpolarizability (β) powder SHG value ranging between 5 and 14×10^{-30} esu but no switching behavior was considered. On the other hand, Nakatani, Delaire, and co-workers^{14–16} investigated the NLO switching behavior of different anils, which crystallize in noncentrosymmetric space groups and exhibit photochromism in the crystalline state.¹⁷ In the present theoretical study, these investigations are extended by considering different sets of substituents and by determining factors governing the amplitude of the second-order NLO responses and their contrast between the two tautomeric forms. Furthermore, this study is included in a broader study aimed at designing efficient NLO switches by integrating organic synthesis, optical characterization, and theoretical interpretations.^{15,18–22} After summarizing the key theoretical and computational aspects in section 2, the results are presented in

* To whom correspondence should be addressed.

(a) 4,4'-substituted *N*-salicylideneanilines

(b) salicylidenemethylamine

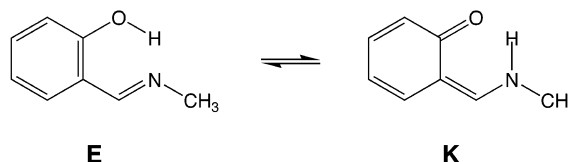


Figure 1. Enol (E) and keto (K) tautomeric forms of Schiff bases with intramolecular hydrogen bond: (a) *N*-salicylideneaniline ($R = H$, $R' = H$), **1**; *N*-salicylidene-4-bromoaniline ($R = Br$, $R' = H$), **2**; 4'-amino-*N*-salicylidene-4-bromoaniline ($R = Br$, $R' = NH_2$), **3**; 4'-amino-*N*-salicylideneaniline ($R = H$, $R' = NH_2$), **4**; 4'-amino-*N*-salicylidene-4-nitroaniline ($R = NO_2$, $R' = NH_2$), **5**; 4'-cyano-*N*-salicylideneaniline ($R = H$, $R' = CN$), **6**; *N*-salicylidene-4-formyl-aniline ($R = CHO$, $R' = H$), **7**; 4'-hydroxy-*N*-salicylideneaniline ($R = H$, $R' = OH$), **8**; *N*-salicylidene-4-aminoaniline ($R = NH_2$, $R' = H$), **9** (b) salicylidenemethylamine, **10**.

section 3: first, the geometrical and thermodynamics aspects and then the NLO properties.

2. Methodology and Computational Procedure

Geometry optimizations of the equilibrium structures and the transition states were performed using Møller-Plesset second-order perturbation theory (MP2/6-31G** and MP2/6-31+G**) with a gradient convergence threshold of 1×10^{-5} hartree bohr⁻¹. Additional Hartree–Fock (HF/6-31G**) and density functional theory (B3LYP/6-31G** and B3LYP/6-31+G**) calculations were also carried out. The nature of the stationary points was verified by calculating the vibrational frequencies. The Hessian matrix contains positive eigenvalues for minima and a single negative eigenvalue for transition states. Predictions of reaction dynamics critically depend on the reaction barrier, i.e., the difference in energy between the transition state and minima. We carried out single-point calculations at the MP4/6-31G**//MP2/6-31G** and MP4/6-31+G**//MP2/6-31+G** levels to validate the accuracy of the barrier height, where computationally feasible. In the MP2 and MP4 calculations, the core occupied orbitals were not correlated.

The values of Gibbs free energies (ΔG) and activation barriers (ΔG^\ddagger) were calculated for a temperature of 298.15 K by the formulas $\Delta G = \Delta H - T\Delta S$ and $\Delta G^\ddagger = \Delta H^\ddagger - T\Delta S^\ddagger$, respectively. To estimate enthalpy values, thermal corrections calculated at the MP2/6-31G** and MP2/6-31+G** levels were added to the calculated total energies. The entropy values were evaluated from the vibrational frequency calculations at the same level of approximation. To estimate the effect of the medium (methanol or water) on the relative stabilities of the tautomers and on the barrier height of tautomerization, single-point calculations using the polarizable continuum model (PCM)²³ were achieved.

First hyperpolarizability tensors were evaluated using (i) the time-dependent Hartree–Fock (TDHF) approach,²⁴ which allows to determine energy derivatives with respect to a perturbing static or dynamic electric field, by solving iteratively the perturbed TDHF equations order by order, and (ii) the MP2/finite field approach²⁵ in order to estimate the importance of correlation effects on these properties. In the latter case, a finite differentiation procedure is employed and combined with the

Romberg procedure to improve the accuracy on the numerical derivatives. These first hyperpolarizability calculations were performed on the MP2/6-31G** optimized geometries, and we checked that when using the other geometry optimization methods mentioned above no significant changes in the hyperpolarizabilities appear. A standard wavelength of 1064 nm was considered in all of the TDHF calculations. To account for frequency dispersion at the MP2 level, the multiplicative correction scheme has been applied. It consists of multiplying the static MP2 value by the TDHF/CPHF ratio, the CPHF (coupled-perturbed Hartree–Fock) scheme being the static equivalent of the TDHF method

$$\beta_{MP2}(-2\omega; \omega, \omega) \approx \beta_{MP2}(0; 0, 0) \times \frac{\beta_{TDHF}(-2\omega; \omega, \omega)}{\beta_{CPHF}(0; 0, 0)} \quad (1)$$

Two measurable second-order NLO responses, derived from specific sums of the first hyperpolarizability tensor components, were determined. The first one corresponds to the projection of the vector part of β on the dipole moment vector, which can be obtained experimentally from electric field induced second harmonic generation (EFISHG) measurements

$$\beta_{||}(-2\omega; \omega, \omega) = \beta_{||} = \frac{3}{5} \sum_i \frac{\mu_i}{||\mu||} \sum_j (\beta_{ijj} + \beta_{jij} + \beta_{jji}) = \frac{3}{5} \sum_i \frac{\mu_i \beta_i}{||\mu||} \quad (2)$$

In eq 2, $||\mu||$ is the norm of the dipole moment and μ_i and β_i the components of the μ and β vectors. The second property is related to the hyper-Rayleigh scattering intensity for plane-polarized incident light and observation made perpendicular to the propagation plane without polarization analysis of the scattered beam

$$\beta_{HRS}(-2\omega; \omega, \omega) = \sqrt{\{\langle \beta_{zzz}^2 \rangle + \langle \beta_{xzz}^2 \rangle\}} \quad (3)$$

whereas the associated depolarization ratio (DR) is given by

$$DR = \frac{\langle \beta_{zzz}^2 \rangle}{\langle \beta_{xzz}^2 \rangle} \quad (4)$$

TABLE 1: Gibbs Energies (kcal mol⁻¹) of Reaction [ΔG_{298}] and of Activation [ΔG_{298}^\ddagger] for the E \rightleftharpoons K Reaction of Salicylidene-methylamine (10) as Well as Imaginary Frequency (cm⁻¹) of the Transition State Calculated at Different Levels of Theory^a

computational level	ΔG_{298}	ΔG_{298}^\ddagger (forward)	ΔG_{298}^\ddagger (reverse)	ν^\ddagger
HF/6-31G**	7.91	12.02	4.11	1640i
MP2/6-31G**	8.11	7.77	-0.34	315i
B3LYP/6-31G**	4.39	3.41	-0.98	1026i
MP2/6-31+G**	7.15	6.52	-0.63	466i
B3LYP/6-31+G**	3.83	3.12	-0.71	955i
MP4/6-31G**//MP2/6-31G**	8.19	8.47	0.28	
MP4/6-31+G**//MP2/6-31+G**	9.35	9.41	0.06	
PCM/MP2/6-31G**//MP2/6-31G** ^b	4.33	4.99	0.66	
PCM/MP2/6-31+G**//MP2/6-31+G** ^b	3.39	4.15	0.76	
PCM/MP2/6-31G**//MP2/6-31G** ^c	4.17	4.91	0.74	
PCM/MP4/6-31G**//MP2/6-31G** ^c	3.09	4.15	1.06	
PCM/MP2/6-31+G**//MP2/6-31+G** ^c	3.30	4.15	0.85	
PCM/MP4/6-31+G**//MP2/6-31+G** ^c	2.17	3.53	1.36	

^a Both forward and reverse activation barriers are given. ^b In methanol. ^c In water.

$\langle\beta_{zzz}\rangle$ and $\langle\beta_{xzz}\rangle$ correspond to orientational averages of the β tensor components, and their full expressions can be found in ref 26 (without assuming Kleinman's conditions) together with more details about the HRS experiment. The depolarization ratio (DR) is indicative of the geometry of the part of the molecule responsible for the NLO response, referred to as the NLO-phore (in 1D donor-acceptor systems, DR = 5, whereas it amounts to 3/2 for octupolar compounds). The reported β values are consistent with the power series expansion of the field-dependent dipole moment (convention B). Several basis sets were used in the β calculations, including 6-31G*, 6-31+G*, 6-311+G*, cc-pvdz, cc-pvtz, aug-cc-pvdz, and aug-cc-pvtz. The calculations were carried out using the GAMESS²⁷ (geometry optimization of K and E forms as well as of TS; single point MP4//MP2 calculations) and the Gaussian program²⁸ (version 98 for single-point PCM calculations and version 03 for first hyperpolarizability calculations).

3. Results and Discussion

3.A. Molecular Structures and Thermodynamics Analysis.

As a first step for theoretically addressing the thermodynamics and kinetics of the E \rightleftharpoons K equilibrium for compounds 1–9, the model salicylidene-methylamine compound 10 was studied in details at different computational levels. The two tautomeric forms of 10 were found to coexist in methanol²⁹ as well as in acetonitrile,³⁰ typical examples of protic and aprotic solvents, indicating that the ΔG and ΔG^\ddagger should not be too large. The computational results are presented in Table 1, whereas those for the substituted *N*-salicylideneanilines, in Table 2. At all levels of approximation, the E form is the most stable.

Considering compound 10, using the MP4//MP2 value as reference, the B3LYP approach underestimates the ΔG_{298} value by more than 50%, whereas the HF and MP2 approaches underestimate it by 1 kcal mol⁻¹ or less. Including solvent effects via the PCM scheme reduces ΔG_{298} substantially with respect to the gas-phase values. Similar conclusions can be drawn for the activation Gibbs energy [ΔG_{298}^\ddagger (forward)], with the exception that the HF method overestimates it by about 50%. This overestimation is not surprising, owing to the fact that accounting for electron correlation is necessary for a reasonable prediction of the activation energies, and that the contribution of the correlation energy is usually larger for transition structures than for equilibrium structures. Besides using the MP4//MP2 level of approximation (and the HF scheme), the activation Gibbs energy for the reverse reaction is always negative when

TABLE 2: Gibbs Energy of Reaction [ΔG_{298} (kcal mol⁻¹)] and of Activation [ΔG_{298}^\ddagger (kcal mol⁻¹)] for the E \rightleftharpoons K Reaction of Substituted *N*-Salicylideneanilines 1–5 and 7–8 Calculated at Different Levels of Theory, Imaginary Frequency (ν^\ddagger , Evaluated at the MP2 Level without Considering the Solvent, cm⁻¹) of the Transition State, and Difference in Dipole Moment (D) between the Tautomeric Forms [$\Delta\mu = \mu(K) - \mu(E)$]

compounds	MP4/6-31G**// MP2/6-31G**		PCM/MP2/6-31G**// MP2/6-31G** ^a		$\Delta\mu$
	ΔG_{298}	ΔG_{298}^\ddagger (ν^\ddagger)	ΔG_{298}	ΔG_{298}^\ddagger	
1	8.02	8.24 (265i)	6.35	6.66	-1.29
2	8.12	8.53 (173i)	6.71	7.43	-0.40
3	6.66	6.27 (632i)	6.29	5.47	0.46
4	6.40	6.05 (656i)	5.24	4.86	-0.35
5	5.36	6.14 (739i)	6.18	6.21	0.36
7	8.13	8.01 (417i)	8.57	8.34	0.16
8	7.46	7.66 (467i)	5.54	5.40	1.52

^a In methanol.

the solvent effects are not taken into account. Negative enthalpies of activation have also been reported by Fabian et al.³¹ in a B3LYP investigation of hydroxynaphthaldehyde anils. In any case, the activation energy is small for the reverse reaction, demonstrating the weak stability of the K form, which can easily convert to the E form. Together with a substantial (relative) stabilization of the K form, including solvent effects reduces the activation barrier and makes them positive for both the forward and reverse paths. Moreover, no major differences are observed when switching from water ($\epsilon = 78.39$) to methanol ($\epsilon = 32.63$). For computational reasons and because the MP4//MP2 and MP2 results are close, the investigation of bigger substituted *N*-salicylideneanilines is limited to MP4/6-31G**//MP2/6-31G** and PCM/MP2/6-31G**//MP2/6-31G** calculations.

Table 2 summarizes the main thermodynamic and kinetic data for the tautomeric equilibrium of compounds 1–9, in fact, with the exception of compounds 6 and 9 for which a stable K form could not be obtained. These unstable-K situations correspond to cases where R is a donor group (D) or R' is an acceptor (A) group, a stable K form is also lacking for R/R' = D/A as found from calculations not reported here, and are characterized by a E form presenting a shorter N1...O15 distance (Table 3). The ΔG_{298} values are smaller than for the reference compound 10 at the MP4/6-31G**//MP2/6-31G** level, whereas at the PCM/MP2/6-31G**//MP2/6-31G** they are 50% smaller. ΔG_{298} is particularly influenced by the presence of the NH₂ donor group

TABLE 3: Selected Distances (Å) and Torsion Angles (°) for *N*-Salicylideneanilines 1–9 Calculated at the MP2/6-31G Level^a**

	1: R = H, R' = H	2: R = Br, R' = H	3: R = Br, R' = NH ₂	4: R = H, R' = NH ₂	5: R = NO ₂ , R' = NH ₂	6: R = H, R' = CN	7: R = CHO, R' = H	8: R = H, R' = OH	9: R = NH ₂ , R' = H
Enol form									
Enol Form									
N1=C2	1.299 (1.262 ^b)	1.299 (1.292 ^d)	1.301	1.300	1.301	1.299	1.299	1.299	1.299
C2–C3	1.450 (1.450 ^c)	1.449 (1.436 ^d)	1.442	1.444	1.441	1.451	1.449	1.447	1.450
C3–C4	1.417	1.417 (1.422 ^d)	1.418	1.418	1.418	1.420	1.417	1.420	1.417
C4–C5	1.401	1.401 (1.379 ^d)	1.395	1.395	1.395	1.400	1.401	1.396	1.401
C5–C6	1.390	1.390 (1.369 ^d)	1.397	1.397	1.397	1.398	1.390	1.392	1.390
C6–C7	1.401	1.402 (1.356 ^d)	1.409	1.409	1.410	1.408	1.402	1.403	1.401
C6–R'	1.083	1.083	1.395	1.396	1.392	1.435	1.083	1.370	1.083
C7–C8	1.387	1.387 (1.358 ^d)	1.382	1.383	1.382	1.385	1.387	1.386	1.388
C3–C8	1.407	1.408 (1.384 ^d)	1.407	1.407	1.408	1.407	1.408	1.405	1.407
C4–O15	1.350 (1.353 ^c)	1.351 (1.375 ^d)	1.351	1.351	1.351	1.345	1.350	1.349	1.350
O15–H16	0.990	0.989 (0.894 ^d)	0.990	0.991	0.989	0.993	0.988	0.991	0.991
N1–C9	1.414 (1.466 ^b)	1.412 (1.412 ^d)	1.410	1.413	1.409	1.414	1.411	1.413	1.411
C9–C14	1.402	1.402 (1.361 ^d)	1.403	1.403	1.403	1.402	1.402	1.402	1.403
C9–C10	1.401	1.401 (1.426 ^d)	1.401	1.401	1.402	1.401	1.404	1.401	1.401
C10–C11	1.393	1.392 (1.364 ^d)	1.392	1.393	1.390	1.393	1.388	1.393	1.390
C11–C12	1.398	1.397 (1.374 ^d)	1.397	1.398	1.394	1.398	1.403	1.398	1.404
C12–C13	1.396	1.395 (1.402 ^d)	1.395	1.396	1.392	1.396	1.399	1.396	1.403
C13–C14	1.395	1.394 (1.363 ^d)	1.394	1.395	1.393	1.395	1.393	1.395	1.392
C12–R	1.082	1.896 (1.897 ^d)	1.897	1.082	1.468	1.082	1.479	1.082	1.401
N1⋯O15	2.641 (2.598 ^b)	2.646	2.646	2.642	2.649	2.629	2.648	2.641	2.638
C8–C3–C2–N1	179.7	179.2	178.4	178.5	178.2	180.0	179.6	179.2	180.0
C3–C2–N1–C9	177.9	178.0	176.7	176.9	177.3	177.6	177.5	177.6	177.3
C2–N1–C9–C10	138.7	139.0	139.6	139.3	138.3	140.2	137.7	139.2	143.6
Keto form	1: R = H, R' = H	2: R = Br, R' = H	3: R = Br, R' = NH ₂	4: R = H, R' = NH ₂	5: R = NO ₂ , R' = NH ₂	7: R = CHO, R' = H	8: R = H, R' = OH		
Keto Form									
N1–C2	1.326	1.327	1.335	1.333	1.339	1.331	1.329		
C2–C3	1.402	1.402	1.391	1.392	1.388	1.397	1.397		
C3–C4	1.455	1.455	1.464	1.463	1.468	1.459	1.462		
C4–C5	1.437	1.436	1.430	1.431	1.431	1.440	1.431		
C5–C6	1.374	1.374	1.379	1.379	1.378	1.372	1.374		
C6–C7	1.422	1.422	1.435	1.434	1.438	1.425	1.427		
C6–R'	1.084	1.084	1.391	1.393	1.387	1.084	1.370		
C7–C8	1.372	1.372	1.365	1.365	1.363	1.370	1.369		
C3–C8	1.423	1.423	1.427	1.426	1.429	1.427	1.422		
C4=O15	1.281	1.282	1.276	1.276	1.273	1.277	1.278		
N1–H16	1.074	1.081	1.058	1.056	1.053	1.065	1.066		
N1–C9	1.407	1.404	1.401	1.404	1.396	1.402	1.406		
C9–C14	1.401	1.401	1.402	1.401	1.403	1.402	1.401		
C9–C10	1.400	1.401	1.401	1.401	1.404	1.405	1.400		
C10–C11	1.393	1.392	1.392	1.392	1.390	1.387	1.393		
C11–C12	1.397	1.396	1.396	1.397	1.393	1.401	1.397		
C12–C13	1.397	1.396	1.396	1.396	1.393	1.399	1.397		
C13–C14	1.394	1.393	1.393	1.394	1.391	1.391	1.394		
C12–R	1.082	1.894	1.895	1.082	1.467	1.479	1.082		
N1⋯O15	2.492	2.481	2.526	2.531	2.537	2.509	2.510		
C8–C3–C2–N1	179.4	179.2	178.1	178.1	180.0	179.2	178.5		
C3–C2–N1–C9	178.6	178.8	177.7	177.6	179.0	178.8	178.6		
C2–N1–C9–C10	151.6	152.7	153.4	152.8	158.9	155.0	152.3		

^a Available experimental data are given in parentheses. ^b Reference 32a. ^c Reference 32b. ^d Reference 19b.

in R' and to a lesser extent by the NO₂ acceptor group in R, that both lead to a decrease in ΔG_{298} . Going from R = H (**1**) to R = Br (**2**) has a reduced effect on $\Delta G_{298}^{\ddagger}$ but a larger effect on ΔG_{298} when the solvent effects are taken into account: additional calculations performed for R = Cl provide similar results to R = Br. $\Delta G_{298}^{\ddagger}$ is also reduced in presence of the NH₂ group as R' substituent, but when accounting for solvent interactions, this effect is reduced when R = NO₂ (**5**).

For compounds **3**, **4**, and **7** (also **8** at the PCM/MP2//MP2 level), the transition state is lower in energy (smaller G_{298} value) than the K form although a saddle point was located on the potential energy surface (one imaginary frequency). This peculiar ordering of the transition state and K form energies

finds its origin in the fact that the stationary/transition states on the potential energy surface are determined by considering minima/maxima on the energy U_0 surface whereas thermodynamics is based on G_{298} , with $G_{298} = U_0 + \text{ZPVE} + \text{thermal corrections including the entropy term}$. Indeed, the corrections to $\Delta U_0^{\ddagger}(\text{reverse})$ to get $\Delta G_{298}^{\ddagger}(\text{reverse})$ are always negative except for compound **2** and amount to -0.44 , 0.03 , -2.22 , -2.27 , -1.53 , -1.21 , and -1.02 kcal/mol for compounds **1–5**, **7**, and **8**, respectively. In the same order, the $\Delta U_0^{\ddagger}(\text{reverse})$ values are 0.67 , 0.38 , 1.82 , 1.93 , 2.31 , 1.09 , and 1.21 . For compounds **3**, **4**, and **7**, the ZPVE + thermal corrections including the entropy term dominate over the ΔU_0^{\ddagger} term, and

TABLE 4: MP2/6-31G** Mulliken Charge Distribution ($|e|$) for Selected Moieties of the *N*-Salicylideneanilines 1–9

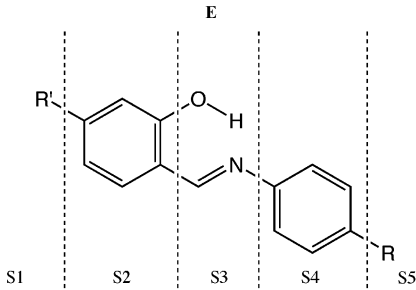
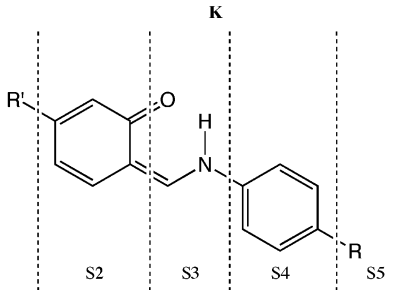
											
S1	S2	S3	S4	S5		S1	S2	S3	S4	S5	
1	0.02	-0.02	-0.14	0.12	0.02	0.01	-0.05	-0.15	0.17	0.02	
2	0.02	0.00	-0.14	0.14	-0.02	0.02	-0.05	-0.15	0.19	-0.01	
3	0.06	-0.01	-0.16	0.13	-0.02	0.07	-0.04	-0.18	0.17	-0.02	
4	0.06	-0.01	-0.16	0.10	0.01	0.06	-0.05	-0.18	0.15	0.02	
5	0.07	0.00	-0.15	0.39	-0.31	0.07	-0.02	-0.16	0.42	-0.31	
6	-0.12	0.08	-0.11	0.13	0.02	/	/	/	/	/	
7	0.02	0.00	-0.13	0.06	0.05	0.02	-0.04	-0.14	0.10	0.06	
8	-0.05	0.03	-0.16	0.16	0.02	-0.05	0.07	-0.15	0.11	0.02	
9	0.02	-0.02	-0.15	0.11	0.04	/	/	/	/	/	

TABLE 5: Basis Set Effects on the TDHF ($\lambda = 1064$ nm) First Hyperpolarizability ($\beta_{||}$ and β_{HRS}), Depolarization Ratio, and Dipole Moment of the E and K Tautomeric Forms of Substituted Schiff Bases and on the Ratio between the K and E First Hyperpolarizabilities^a

compounds	basis sets	E forms				K forms				ratio K/E	
		$\beta_{ }$	β_{HRS}	DR	μ	$\beta_{ }$	β_{HRS}	DR	μ	$\beta_{ }$	β_{HRS}
1 R = R' = H	cc-pvdz	-196.0	194.7	3.17	2.42	-216.9	255.5	2.47	3.98	1.107	1.312
	cc-pvtz	-193.7	183.2	3.18	2.39	-202.5	253.0	2.47	3.97	1.045	1.381
	aug-cc-pvdz	-245.1	199.1	4.02	2.41	-224.7	291.8	2.81	3.98	0.917	1.466
	aug-cc-pvtz	-245.3	196.3	4.08	2.39	-229.6	289.5	2.90	3.97	0.936	1.475
	6-31G*	-186.7	193.7	3.18	2.62	-194.2	241.5	2.43	4.08	1.040	1.247
	6-31+G*	-268.8	232.5	3.90	2.62	-269.5	329.0	2.70	4.18	1.003	1.415
2 R = Br R' = H	6-311+G*	-255.6	219.0	3.87	2.64	-252.6	308.0	2.67	4.15	0.988	1.406
	cc-pvdz	-120.6	160.6	2.72	2.84	-241.4	272.4	2.75	2.96	2.002	1.696
	cc-pvtz	-107.9	169.5	2.83	2.91	-254.6	271.8	2.69	2.98	2.360	1.604
	aug-cc-pvdz	-136.9	189.5	3.67	2.94	-321.2	319.2	3.18	3.00	2.346	1.684
	aug-cc-pvtz	-122.1	191.9	4.02	2.92	-324.4	305.9	3.17	3.00	2.657	1.594
	6-31G*	-65.5	169.4	2.87	3.02	-236.6	252.9	2.60	3.08	3.612	1.493
3 R = Br R' = NH ₂	6-31+G*	-123.7	216.7	3.46	3.05	-346.8	344.8	2.98	3.18	2.804	1.591
	6-311+G*	-135.8	201.8	3.49	3.04	-323.1	323.9	2.96	3.17	2.379	1.605
	cc-pvdz	868.6	848.8	3.81	4.85	-10.6	389.0	2.82	4.26	-0.012	0.458
	cc-pvtz	921.9	876.4	3.91	4.91	24.4	407.2	2.91	4.28	-0.026	0.465
	aug-cc-pvdz	992.9	931.9	4.18	4.89	-20.2	423.8	3.01	4.26	-0.020	0.455
	6-31G*	870.6	868.0	3.94	4.84	8.3	388.7	2.98	4.34	0.010	0.448
4 R = H R' = NH ₂	6-31+G*	1040.8	1026.9	4.15	4.88	-29.7	502.1	3.13	4.38	-0.029	0.489
	6-311+G*	982.8	976.5	4.11	4.88	-19.0	479.8	3.08	4.37	-0.019	0.491
	cc-pvdz	459.5	807.0	3.96	3.11	-266.3	450.7	3.31	3.77	-0.580	0.558
	cc-pvtz	464.8	792.5	4.01	3.10	-252.0	434.9	3.26	3.74	-0.542	0.549
	aug-cc-pvdz	480.9	844.7	4.34	3.08	-313.5	458.7	3.36	3.72	-0.652	0.543
	aug-cc-pvtz	473.0	822.6	4.34	3.09	-316.5	452.1	3.38	3.71	-0.669	0.550
	6-31G*	349.4	784.9	3.94	3.18	-261.5	418.0	3.22	3.93	-0.748	0.533
	6-31+G*	431.9	937.6	4.30	3.19	-378.6	538.1	3.42	3.98	-0.877	0.574
	6-311+G*	426.7	900.7	4.27	3.22	-345.8	518.5	3.38	3.94	-0.810	0.576

^a The geometries were optimized at the HF/6-31G** level of approximation. The β values are given in au ($1.0 \text{ au of } \beta = 3.6213 \times 10^{-42} \text{ m}^4 \text{ V}^{-1} = 3.206361 \times 10^{-53} \text{ C}^3 \text{ m}^3 \text{ J}^{-2} = 8.6392 \times 10^{-33} \text{ esu}$), the dipole moments in D.

the activation barrier, $\Delta G_{298}^{\ddagger}(\text{reverse})$, is negative. The transition states of compounds **3**, **4**, **7**, and **8** are described by large imaginary frequencies (about 600 cm^{-1}), like in compound **5**, whereas for compounds **1** and **2**, the frequencies are much smaller, demonstrating a smoother potential energy surface. A global trend can however be deduced: an acceptor group in R

leads to an increase of ΔG_{298} , whereas a donor group in R' has the opposite effect. The $\Delta G_{298}^{\ddagger}$ values follow the ΔG_{298} trend.

The optimized geometries have then been analyzed in order to make correlations with the energy differences (Table 3). Compounds **1** and **2** present essentially the same geometries. Going from these compounds without strong D/A substituents

TABLE 6: First Hyperpolarizability, Depolarization Ratio, Dipole Moment, and Angle (θ) between the Dipole Moment and First Hyperpolarizability Vectors of the E and K Tautomeric Forms of Substituted Schiff Bases Obtained at Different Levels of Approximation with cc-pvdz Basis Set for the MP2/6-31G Optimized Geometries^a**

compounds	methods	E forms				K forms			
		$\beta_{ }$	β_{HRS}	DR	μ (θ)	$\beta_{ }$	β_{HRS}	DR	μ (θ)
1 R = R' = H	CPHF	−178.3	180.2	2.93	1.08	−337.2	306.2	2.80	1.68
		(−236.1)	(209.8)			(−386.7)	(347.5)		
	TDHF (λ = 1064 nm)	−218.2	211.4	3.09		−498.7	434.5	3.16	
	FF/MP2	−361.4	371.5	4.87	0.90 (133)	−229.3	222.6	2.58	1.47 (171)
		(−397.7)	(401.5)			(−239.5)	(274.7)		
	MP2 (λ = 1064 nm)	−442.3	435.8			−339.1	315.9		
2 R = Br R' = H	CPHF	−132.9	152.1	2.66	1.24	−277.6	283.0	2.48	1.37
	TDHF (λ = 1064 nm)	−178.4	186.0	2.88		−412.7	414.7	2.74	
	FF/MP2	34.5	263.9	4.40	0.77 (85)	−114.5	217.2	2.90	0.99 (118)
	MP2 (λ = 1064 nm)	46.3	322.7			−170.2	318.3		
3 R = Br R' = NH ₂	CPHF	528.3	628.5	3.48	1.92	18.4	518.7	2.97	1.73
	TDHF (λ = 1064 nm)	740.4	834.5	3.74		8.9	626.8	3.26	
	FF/MP2	1495.7	1317.5	4.57	1.47 (36)	120.0	379.7	2.74	1.24 (73)
	MP2 (λ = 1064 nm)	2096.2	1749.3			58.0	458.8		
4 R = H R' = NH ₂	CPHF	200.8	625.0	3.71	1.32	−320.5	556.4	3.30	1.57
	TDHF (λ = 1064 nm)	286.4	808.0	3.91		−407.0	676.0	3.60	
	FF/MP2	692.4	1258.6	4.68	0.97 (67)	−209.5	531.7	3.50	1.08 (108)
	MP2 (λ = 1064 nm)	987.6	1627.1			−266.0	646.0		
5 R = NO ₂ R' = NH ₂	CPHF	1771.9	1444.1	3.96	8.59	1548.6	1455.9	3.85	7.74
	TDHF (λ = 1064 nm)	2621.5	2080.8	4.21		2346.7	2124.6	4.20	
	FF/MP2	3681.3	2716.8	4.78	6.44 (19)	2557.9	2055.4	4.44	5.94 (27)
	MP2 (λ = 1064 nm)	5446.4	3914.6			3876.2	2999.4		
6 R = H R' = CN	CPHF	68.1	149.7	4.25	6.61	/			
	TDHF (λ = 1064 nm)	212.4	260.0	4.80					
	FF/MP2	−275.4	190.4	5.23	6.41 (170)				
	MP2 (λ = 1064 nm)	−859.0	330.7						
7 R = CHO R' = H	CPHF	282.2	556.6	3.80	5.37	−46.6	748.9	3.74	5.59
	TDHF (λ = 1064 nm)	420.2	746.9	4.08		−37.5	1140.0	4.25	
	FF/MP2	741.9	1081.8	4.94	3.57 (62)	−3.6	991.6	4.38	3.75 (90)
	MP2 (λ = 1064 nm)	1104.7	1451.7			−2.9	1509.4		
8 R = H R' = OH	CPHF	−199.2	416.7	3.51	4.24	−447.6	439.3	3.25	5.80
	TDHF (λ = 1064 nm)	−236.9	509.9	3.68		−580.4	542.7	3.59	
	FF/MP2	−255.7	842.7	4.73	3.38 (102)	−388.7	400.5	3.58	4.53 (139)
	MP2 (λ = 1064 nm)	−304.1	1031.2			−504.0	494.8		
9 R = NH ₂ R' = H	CPHF	86.9	414.7	4.71	4.02	/			
	TDHF (λ = 1064 nm)	183.6	644.6	4.68					
	FF/MP2	306.5	443.5	4.62	4.05 (61)				
	MP2 (λ = 1064 nm)	647.6	689.4						

^a The β values are given in au, the dipole moments in D, and the angles in degrees. The values in parentheses have been obtained using the 6-31+G* basis set.

to compound **5**, the changes in geometry are first associated with the mesomeric donor character of the NH₂ group, which increases the quinoid character of the phenyl ring. Then, the bond length alternation (BLA) in the bridge between the two rings, estimated as $BLA = (d_{3-2} + d_{1-9} - 2d_{2-1})/2$, goes from 0.13 Å in **1** to 0.11 Å in **5** for the E form. For **7** and **8**, which contain an acceptor in R or a donor in R', the effect is smaller and located mostly at the side of the substitution. For the K form, the BLA is smaller and goes from 0.08 Å in **1** to 0.05 Å in **5**. This larger decrease of BLA between the E and K forms of 4'-amino-*N*-salicylidene-4-nitroaniline accounts for a larger increase of electron delocalization and of stabilization of the K form. The values of the torsion angles further show that the imine is conjugated with the salicylidene ring, whereas the other ring is twisted by about 40° with respect to a planar situation. Upon transformation from the E to the K form, the system gets more planar with a deviation from planarity reduced to less than 30°.

The sums of the net MP2 Mulliken atomic charges in different fragments (Si, with $i = 1-5$) for compounds **1-9** are collected

in Table 4. For both forms, the central moiety (S3) bears a negative charge. This excess of electron is related to positive S4 (or S4 + S5) fragments. Although the effect is small, the K form is characterized by a larger negative charge on S2 and a larger positive charge on S4 than in the E form. The presence of D and/or A groups has mostly a direct influence on the ring on which the substituents are attached, demonstrating that there is no real charge transfer between R and R', even in the case of compound **5**. Indeed, comparing compounds **4** and **5**, the charge on the R' = NH₂ group is mostly identical.

3.B. Nonlinear Optical Properties. Basis set effects on the first hyperpolarizabilities, depolarization ratios, and dipole moments have first been addressed at the TDHF level of approximation for compounds **1-4** (Table 5). In particular, the effect of adding diffuse functions has been studied. Adding diffuse functions to the cc-pvdz, cc-pvtz, or 6-31G* basis set leads to (i) small variations of the dipole moment ($\leq 3\%$), (ii) an increase of $\beta_{||}$ that can be larger than for μ and that can be associated with important variations of the $\beta_{||}(K)/\beta_{||}(E)$ ratios, (iii) smaller variations of the β_{HRS} values than of their EFISH

TABLE 7: K/E First Hyperpolarizability ($\beta_{||}$ and β_{HRS}) Ratios for Substituted Schiff Bases Calculated at Different Levels of Approximation with the cc-pvdz Basis Set for MP2/6-31G Optimized Geometries^a**

compounds	methods	$\beta_{ }$	β_{HRS}
1	CPHF	1.89 (1.64)	1.70 (1.66)
	TDHF ($\lambda = 1064$ nm)	2.29	2.06
	FF/MP2	0.63 (0.60)	0.60 (0.68)
	MP2 ($\lambda = 1064$ nm)	0.77	0.72
2	CPHF	2.09	1.86
	TDHF ($\lambda = 1064$ nm)	2.31	2.23
	FF/MP2	-3.32	0.82
	MP2 ($\lambda = 1064$ nm)	-3.68	0.99
3	CPHF	0.03	0.83
	TDHF ($\lambda = 1064$ nm)	0.01	0.75
	FF/MP2	0.08	0.29
	MP2 ($\lambda = 1064$ nm)	0.03	0.26
4	CPHF	-1.60	0.89
	TDHF ($\lambda = 1064$ nm)	-1.42	0.84
	FF/MP2	-0.30	0.42
	MP2 ($\lambda = 1064$ nm)	-0.27	0.40
5	CPHF	0.87	1.01
	TDHF ($\lambda = 1064$ nm)	0.90	1.02
	FF/MP2	0.50	0.76
	MP2 ($\lambda = 1064$ nm)	0.52	0.77
7	CPHF	-0.17	1.35
	TDHF ($\lambda = 1064$ nm)	-0.09	1.53
	FF/MP2	-0.005	0.92
	MP2 ($\lambda = 1064$ nm)	-0.003	1.04
8	CPHF	2.25	1.05
	TDHF ($\lambda = 1064$ nm)	2.45	1.06
	FF/MP2	1.66	0.48
	MP2 ($\lambda = 1064$ nm)	1.66	0.48

^a The values in parentheses have been obtained using the 6-31+G* basis set. There is no result for compounds **6** and **9** since they do not present a stable K form.

analog, and (iv) an increase of the depolarization ratios of the order of 10% except for **1**(E) and **2**(E) where it is 25–35% larger. In general, the differences are larger for $\beta_{||}$ than β_{HRS} , which can be attributed to its directional character (eq 2). Besides two cases [the $\beta_{||}(K)/\beta_{||}(E)$ ratio of **2** and the $\beta_{||}(K)$ value of **3**], adding a third set of valence functions (from 6-31+G* to 6-311+G* as well as from cc-pvdz to cc-pvtz) changes the different properties by less than 10%. In most cases there is also a very good agreement between the results obtained using the 6-31+G*, 6-311+G*, aug-cc-pvdz, and aug-cc-pvtz basis sets. Moreover, the cc-pvdz basis set performs better than the 6-31G* basis set. In particular, adding diffuse functions to cc-pvdz has a smaller impact than adding diffuse functions on the 6-31G* basis set, demonstrating that in many cases, and in particular for the $\beta(K)/\beta(E)$ ratios, the cc-pvdz basis set is a good compromise between efficiency and accuracy.

Tables 6 and 7 report data obtained at the MP2 level of approximation on geometries optimized using the MP2/6-31G** method, not only static first hyperpolarizability values but also estimated dynamic quantities using eq 1. Including electron correlation at the MP2 level leads to a reduction of the dipole moment, except for **9**(E), as already found for other push–pull π -conjugated compounds,³³ whereas the impact on the first hyperpolarizability is more complex. Indeed, when R is not a strong acceptor group, the $\beta_{HRS}(K)$ values decrease, whereas the $\beta_{HRS}(E)$ quantities increase for compounds **1–9**. This results in a decrease of the $\beta_{HRS}(K)/\beta_{HRS}(E)$ ratio (Table 7) and inverts the conclusions about the relative magnitude of the first

hyperpolarizabilities of the two tautomeric forms. In most of the cases, the behavior of $\beta_{||}$ and $\beta_{||}(K)/\beta_{||}(E)$ with respect to electron correlation is similar. Except for compound **9**, by including electron correlation at the MP2 level, the depolarization ratios increase substantially for the E form (from 26 to 66%), figuring out a β tensor dominated by a few components. For the K forms, there is no systematic effect. Indeed, the DR increases for compounds **2**, **4**, **5**, **7**, and **8** (up to 17%) but decreases for compounds **1** and **3** (up to 8%).

To further analyze the effects of the substituents on the second-order NLO responses, the μ and β vectors are sketched in the molecular frame in Figure 2, whereas the angles they form are also reported in Table 6. Figure 2 highlights that, with the exception of compound **9**(E) having a donor group in the R position, the β vectors of the E forms are always oriented from the “aniline to salicylidene” rings while their amplitude varies over more than 1 order of magnitude. For the K forms, the situation is similar except for compound **2**. On the other hand, the substituents have a strong impact on the orientation of the dipole moment of both forms.

Considering the dynamic MP2 results and using the nonsubstituted compound **1** as the reference, the addition of a Br substituent (compound **2**) reduces substantially the $\beta_{||}$ response of the E form, whereas the decrease is smaller for the K form. This is mostly due to the reorientation of the dipole moment, which almost forms a $\pi/2$ angle with β in **2**(E). Adding an amino group (compound **4**) changes the sign of $\beta_{||}(E)$, of which the amplitude increases by about 100% with respect to the **1**(E) compound. On the contrary, $\beta_{||}(K)$ is smaller for compound **4** than for compound **1**. Note that, in the **1–2–4** sequence, the θ angle gets smaller (the μ and β vectors tend to become parallel) but its value is smaller for the E than the K forms. This illustrates how the donor effects can be totally different on the $\beta_{||}$ values of the two tautomeric forms. Adding an acceptor leads to positive $\beta_{||}(E)$ if it is placed in R (**7**) and negative $\beta_{||}(E)$ if in R' (**6**). The same is found with a donor (**8** and **9**), at least if the donor in R' is not too strong (**4**). For the K form, $\beta_{||}$ is more negative for compound **8** than for compound **4**, i.e., the largest value is obtained for the weaker donor group because θ is larger. Combining both the Br and NH₂ substituents leads to a substantial increase of $\beta_{||}(E)$ but a decrease of $\beta_{||}(K)$. This is again consistent with a gradual decrease of θ from **1** to **2** and from **1** to **4** and the fact that $\theta(\mathbf{1}(E)) < \theta(\mathbf{1}(K))$. Then, adding the NH₂/NO₂ donor/acceptor pair (compound **5**), i.e., replacing the weak Br acceptor by the strong NO₂ acceptor, is associated with substantial increases of both $\beta_{||}(E)$ and $\beta_{||}(K)$.

These chemical substitution effects lead therefore to substantial modulations of the $\beta_{||}(K)/\beta_{||}(E)$ ratio. Indeed, it starts at a value of 0.77 for compound **1**. Following the increasing order of θ variations, the $\beta_{||}(K)/\beta_{||}(E)$ ratio becomes larger than unity for compound **8** and compound **2**, though for the latter the sign is negative. This corresponds to systems with a donor in R' or an acceptor in R. If the donor in R' (compound **4**) or the acceptor in R (compound **7**) becomes stronger, the amplitude of the ratio continues to decrease. Combining donor and acceptor groups in an appropriate way (compound **3**) leads to a positive, although small, ratio. Finally, in compound **5**, this ratio is again positive but still smaller than for compound **1**. Thus, going from compound **1** to compound **5**, the orientation of the dipole moment with respect to the first hyperpolarizability vector has changed by about 120–140°, ranging from almost antiparallel to almost parallel.

In the case of the hyper-Rayleigh response, adding a Br atom reduces $\beta_{HRS}(E)$ by about 25%. When adding an amino group

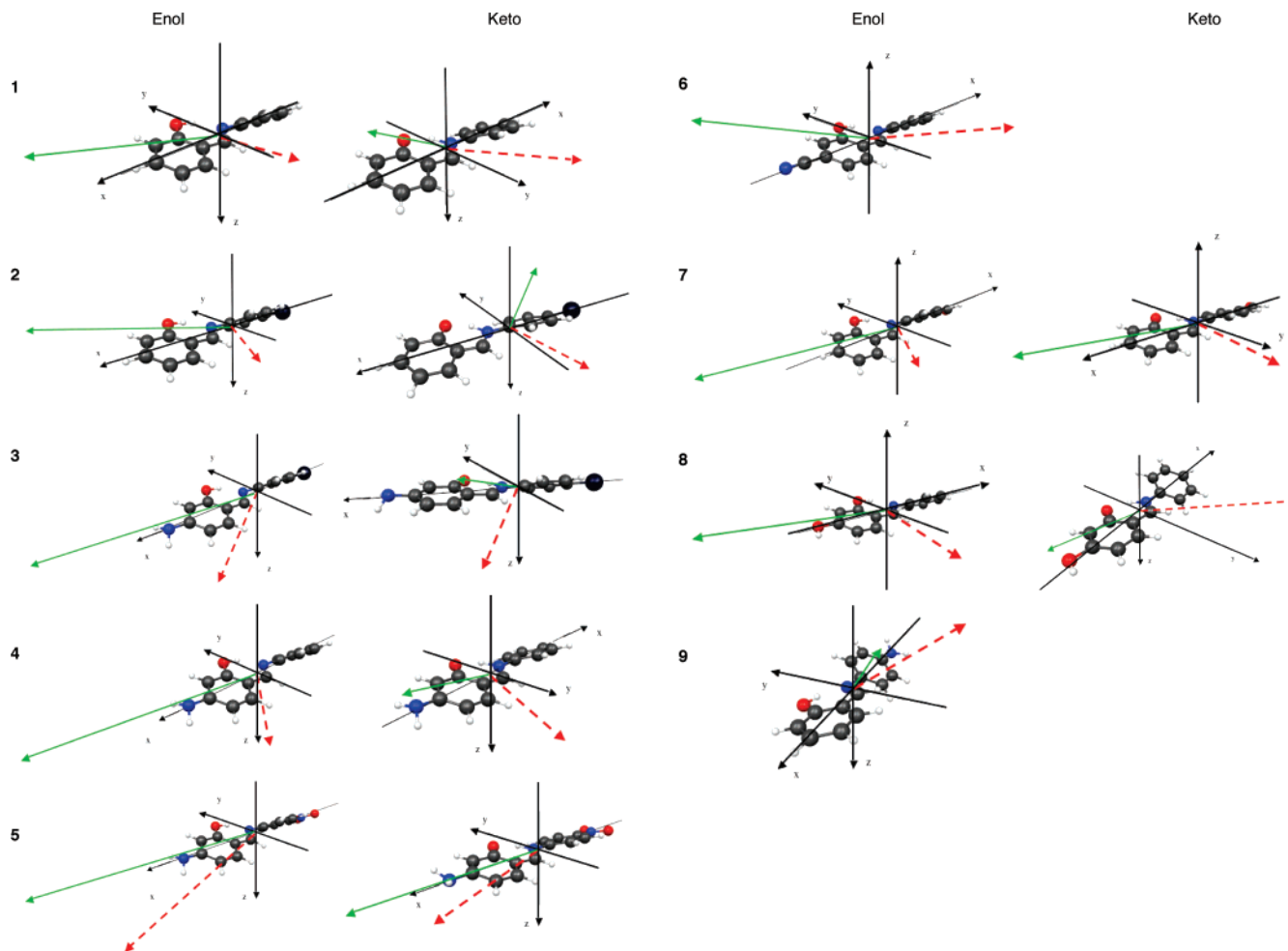


Figure 2. Sketch of the MP2/cc-pvdz dipole moment (red dotted line) and first hyperpolarizability (green full line) vectors for the E (left) and K (right) forms of compounds 1–9 in the molecular frame. For μ , the length of the arrows is proportional to the vector norm (thus consistent for all species). For β , the length of the arrow has been multiplied by a scaling factor, which is the same for the two forms of a given compound. To get consistent norm for all systems, the lengths should be multiplied by 2:1:4:4:8:1:4:3:2 for compounds 1–9, respectively.

(compound 4), $\beta_{\text{HRS}}(\text{E})$ substantially increases and further increases when $\text{R} = \text{Br}$ (compound 3). Thus, like for β_{H} , the effects of the Br atom depend on the presence of the amino group but the effect on β_{HRS} is reverted. A further increase of $\beta_{\text{HRS}}(\text{E})$ accompanies the presence of the NH_2/NO_2 donor/acceptor pair, demonstrating that the increase in β follows the order of the D/A strengths. Moreover, an acceptor R group (7) leads to larger $\beta_{\text{HRS}}(\text{E})$ than with $\text{R}' = \text{acceptor}$ only for the weaker acceptor group (8). Comparing compounds 4 and 9, the optimal position for a donor group is in R' rather than R while, it is preferential to place an acceptor in R, as evidenced by the small β_{HRS} value in 6(E). In the case of the K tautomeric form, adding a Br atom has a negligible impact on the β_{HRS} of compound 1 whereas it leads to a reduction of β_{HRS} of compound 4 (with respect to 3) by about 30%. However, in the presence of a strong R donor group (compound 5), $\beta_{\text{HRS}}(\text{K})$ substantially increases but β_{HRS} remains smaller than for the E form. In fact, except when $\text{R} = \text{CHO}$, $\beta_{\text{HRS}}(\text{K}) < \beta_{\text{HRS}}(\text{E})$, and thus, from comparing compounds 7 and 8, it turns out that an acceptor in R has a larger beneficial effect on $\beta_{\text{HRS}}(\text{K})$ than having a donor in R' .

As a consequence, the $\beta_{\text{HRS}}(\text{K})/\beta_{\text{HRS}}(\text{E})$ ratio amounts to 0.72 for compound 1 but decreases to 0.48 for compound 8 and to 0.40 for compound 4, i.e., with the donor strength of the R' substituent. When R is an acceptor group, the $\beta_{\text{HRS}}(\text{K})/\beta_{\text{HRS}}(\text{E})$ ratio increases to 0.99 (compound 2) and 1.04 (compound 7).

Combining these donor acceptor effects on the same system leads to a smaller ratio for compound 3 than for compound 5. For compound 3, the donor effect of the NH_2 group is enhanced by the presence of the Br atom, whereas for compound 5, it is balanced by the NO_2 group. Indeed, adding a Br in R to get compound 3 reduces $\beta_{\text{HRS}}(\text{K})$ but enhances $\beta_{\text{HRS}}(\text{E})$.

In most cases, the differences between the first hyperpolarizabilities (β_{H} or β_{HRS} , or both) of the tautomeric forms are sufficiently large to be detected and to present a clear contrast. The K/E β ratios obtained for compound 1 are in good qualitative agreement with the powder SHG measurements of ref 14a, although in that case the SHG intensity decreases when λ increases.

4. Conclusion and Further Discussions

The keto–enol tautomerization equilibrium, and, more particularly, the keto-amine/enol-imine equilibrium, has been investigated for a series of substituted salicylideneanilines in view of designing compounds with large contrast of first hyperpolarizabilities. From the initial structural and energy characterization, one has observed that substituting the salicylidene ring by an acceptor group or the other ring by a donor prevents the K form to be stable, whereas in the other cases, the K form can easily be converted to the E form due to small activation barrier, figuring out in most cases that the K form is metastable.

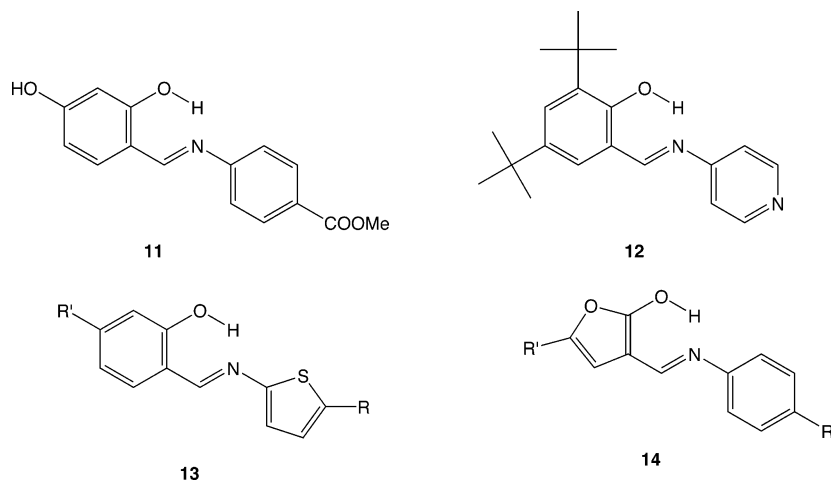


Figure 3. Enol forms of Schiff bases: 4'-hydroxy-*N*-salicylidene-amino-4-(methylbenzoate), **11**; 3,5-di-*tert*-butyl-*N*-salicylidene-4-aminopyridine, **12**; as well as two structures built from heteroaromatic cycles (**13** and **14**).

The different compounds present a sufficiently large contrast of β between the E and K forms to allow its detection for at least one type of second-order NLO measurements (EFISH or HRS). Moreover, the variations of first hyperpolarizability, $\beta_{||}$ and β_{HRS} , with substituents have been rationalized by correlating their amplitudes with their position and donor/acceptor strengths. Irrespective of the tautomeric form, the largest β values are generally associated with species bearing a donor in R' and an acceptor in R. In such cases, the E forms present larger β values than the K form. The angle between the dipole moment and the first hyperpolarizability vectors, and therefore $\beta_{||}$, varies substantially with the strength of the donor/acceptor groups, mostly as a result of the dependence of the dipole moment orientation with respect to the molecular frame, whereas the first hyperpolarizability vector is generally oriented toward the salicylidene rings. Although solid-state effects might tune these conclusions,³⁴ these theoretical investigations will help to orient the synthesis of second-order NLO switches toward more promising compounds.

Future work will encompass joint experimental-theoretical characterizations of anils bearing a donor in R' and an acceptor in R position as well as anils containing heteroaromatic cycles (Figure 3). Compounds **11** and **12** have already been prepared by Sliwa et al.,¹⁶ in view of enhancing the β response by incorporating donor/acceptor substituents (**11**) and in view of stabilizing the K form by introducing bulky substituents (**12**). On the other hand, changing the aromatic cycles can also stabilize the K form via variations of the ring aromaticity (**12**–**14**).

Acknowledgment. This study results from scientific cooperations established and supported by the Belgian National Fund for Scientific Research (FNRS), the Commissariat Général aux Relations Internationales (CGRI) of the Communauté française Wallonie-Bruxelles, the Bulgarian Academy of Sciences, and the Centre National de la Recherche Scientifique (CNRS). B.C. thanks the Belgium National Fund for Scientific Research (FNRS) for his research director position. The calculations have been performed on the Interuniversity Scientific Computing Facility (ISCF) installed at the Facultés Universitaires Notre-Dame de la Paix (Namur, Belgium) for which the authors gratefully acknowledge the financial support of the FNRS-FRFC and the "Loterie Nationale" for the convention No. 2.4578.02. and of the FUNDP.

References and Notes

- (1) Feringa, B. L.; Jager, W. F.; de Lange, B. *Tetrahedron* **1993**, *37*, 8267.
- (2) Hadjoudis, E. *Mol. Eng.* **1995**, *5*, 301.
- (3) Enchev, V.; Ugrinov, A.; Neykov, G.D. *J. Mol. Struct. (THEOCHEM)* **2000**, *530*, 223.
- (4) Hadjoudis, E.; Mavridis, I. M. *Chem. Soc. Rev.* **2004**, *33*, 579.
- (5) Amimoto, K.; Kawato, T. J. *Photochem. Photobiol. C: Photochem. Rev.* **2005**, *6*, 207.
- (6) Abou-Zied, O. K.; Jimenez, R.; Romesberg, F. E. *J. Am. Chem. Soc.* **2001**, *123*, 4613.
- (7) (a) *Molecular Switches*; Feringa, B. L., Ed.; Wiley-VCH: Weinheim, Germany, 2001. (b) Lucas, L.; De Jong, J.; Van Esch, J.; Kellogg, R. M.; Feringa, B. L. *Eur. J. Org. Chem.* **2003**, *1*, 155.
- (8) (a) Fujiwara, T.; Harada, J.; Ogawa, K. *J. Phys. Chem. B* **2004**, *108*, 4035.
- (9) (a) Kabak, M.; Elmali, A.; Elerman, Y. *J. Mol. Struct.* **1999**, *477*, 151. (b) Ogawa, K.; Harada, J.; Tamura, I.; Noda, Y. *Chem. Lett.* **2000**, *528*. (c) Chong, J. H.; Sauer, M.; Patrick, B. O.; MacLachlan, M. J. *Org. Lett.* **2003**, *5*, 3823.
- (10) Alarcon, S. H.; Olivieri, A. C.; Gonzalez-Sierra, M. *J. Chem. Soc. Perkin Trans.* **1994**, *2*, 1067.
- (11) (a) Salman, S. R.; Farrant, R. D.; Lindon, J. C. *Spectrosc. Lett.* **1991**, *24*, 1071. (b) Salman, S. R.; Kanber, S. K.; Arsalan, K. L. *Spectrosc. Lett.* **1991**, *24*, 1153. (c) Salman, S. R.; Lindon, J. C.; Farrant, R. D.; Carpenter, T. A. *Magn. Reson. Chem.* **1993**, *31*, 991. (d) Salman, S. R.; Petros, A. G.; Sweatman, B. C.; Lindon, J. C. *Can. J. Appl. Spectrosc.* **1994**, *39*, 1.
- (12) (a) Carles, M.; Mansilla-Koblavi, F.; Tenon, J. A.; N'Guessan, T. Y.; Bodot, H.; *J. Phys. Chem.* **1993**, *97*, 3716. (b) Mansilla-Koblavi, F.; Tenon, J. A.; Toure, S.; Ebby, N. D.; Lapasset, J.; Carles, M. *Acta Crystallogr. C* **1995**, *51*, 1595.
- (13) (a) Bhat, K.; Chang, K. J.; Aggarwal, M. D.; Wang, W. S.; Penn, B. G.; Frazier, D. O. *Mater. Chem. Phys.* **1996**, *44*, 261. (b) Zhang, Y.; Zhao, C. Y.; Fang, W. H.; You, X. Z. *Theor. Chem. Acc.* **1997**, *96*, 129.
- (14) (a) Nakatani, K.; Delaire, J. A. *Chem. Mater.* **1997**, *9*, 2682. (b) Poineau, F.; Nakatani, K.; Delaire, J. A. *Mol. Cryst. Liq. Cryst.* **2000**, *344*, 89.
- (15) Delaire, J. A.; Nakatani, K. *Chem. Rev.* **2000**, *100*, 1817.
- (16) (a) Sliwa, M.; Létard, S.; Malfant, I.; Nierlich, M.; Lacroix, P. G.; Asahi, T.; Masuhara, H.; Yu, P.; Nakatani, K. *Chem. Mater.* **2005**, *17*, 4727. (b) Sliwa, M.; Nakatani, K.; Asahi, T.; Lacroix, P. G.; Pansu, R. B.; Masuhara, H. *Chem. Phys. Lett.* **2007**, *437*, 212.
- (17) (a) Cohen, M. D.; Schmidt, G. M. J.; Flavian, S. J. *Chem. Soc. Chem. Commun.* **1964**, 2041. (b) Lindeman, S. V.; Shklover, V. E.; Struchkov, Y.; Kravcheny, S. G.; Potapov, V. M. *Cryst. Struct. Commun.* **1982**, *11*, 43.
- (18) Houbrechts, S.; Clays, K.; Persoons, A.; Pikramenou, Z.; Lehn, J. M. *Chem. Phys. Lett.* **1996**, *258*, 485.
- (19) (a) Hillebrand, S.; Segala, M.; Buckup, T.; Correia, R. R. B.; Horowitz, F.; Stefani, V. *Chem. Phys.* **2001**, *273*, 1. (b) Rodembusch, F. S.; Buckup, T.; Segala, M.; Tavares, L.; Correia, R. R. B.; Stefani, V. *Chem. Phys.* **2004**, *305*, 155.
- (20) (a) Coe, B. J.; Houbrechts, S.; Asselberghs, I.; Persoons, A. *Angew. Chem. Int. Ed.* **1999**, *38*, 366. (b) Coe, B. J. *Chem. Eur. J.* **1999**, *5*, 2464; (c) Coe, B. J. *Acc. Chem. Res.* **2006**, *39*, 383.

- (21) (a) Sanguinet, L.; Pozzo, J. L.; Rodriguez, V.; Adamietz, F.; Castet, F.; Ducasse, L.; Champagne, B. *J. Phys. Chem. B* **2005**, *109*, 11139. (b) Mançois, F.; Rodriguez, V.; Pozzo, J. L.; Champagne, B.; Castet, F. *Chem. Phys. Lett.* **2006**, *427*, 153. (c) Sanguinet, L.; Pozzo, J. L.; Guillaume, M.; Champagne, B.; Castet, F.; Ducasse, L.; Maury, O.; Soulié, J.; Mançois, F.; Adamietz, F.; Rodriguez, V. *J. Phys. Chem. B* **2006**, *110*, 10672.
- (22) Botek, E.; Spassova, M.; Champagne, B.; Asselberghs, I.; Persoons, A.; Clays, K. *Chem. Phys. Lett.* **2005**, *412*, 274; **2006**, *417*, 282.
- (23) Miertus, S.; Scrocco, E.; Tomasi, J. *Chem. Phys.* **1981**, *55*, 117; (b) Tomasi, J.; Mennucci, B.; Cammi, R. *Chem. Rev.* **2005**, *105*, 2999.
- (24) (a) Sekino, H.; Bartlett, R. J. *J. Chem. Phys.* **1986**, *85*, 976. (b) Karna, S. P.; Dupuis, M. *J. Comp. Chem.* **1991**, *12*, 487.
- (25) Cohen, H. D.; Roothaan, C. C. J.; *J. Chem. Phys.* **1965**, *43*, S34. For an application of this method and the use of Romberg procedure, see: (b) Champagne, B.; Kirtman, B. In *Handbook of Advanced Electronic and Photonic Materials and Devices*; Nalwa, H. S., Ed.; Academic Press: New York, 2001; Vol. 9, Chapter 2, p 63.
- (26) Bersohn, R.; Pao, Y. H.; Frisch, H. L. *J. Chem. Phys.* **1966**, *45*, 3184. Clays, A. P. *Acc. Chem. Res.* **1998**, *31*, 675.
- (27) Schmidt, M. W.; Baldrige, K. K.; Boatz, J. A.; Elbert, S. T.; Gordon, M. S.; Jensen, J. H.; Koseki, S.; Matsunaga, N.; Nguyen, K. A.; Su, S.; Windus, T. L.; Dupuis, M.; Montgomery, J. A. *J. Comput. Chem.* **1993**, *14*, 1347.
- (28) (a) Frisch, M. J.; Trucks, G. W.; Schlegel, H. B.; Scuseria, G. E.; Robb, M. A.; Cheeseman, J. R.; Zakrzewski, V. G.; Montgomery, J. A., Jr.; Stratmann, R. E.; Burant, J. C.; Dapprich, S.; Millam, J. M.; Daniels, A. D.; Kudin, K. N.; Strain, M. C.; Farkas, O.; Tomasi, J.; Barone, V.; Cossi, M.; Cammi, R.; Mennucci, B.; Pomelli, C.; Adamo, C.; Clifford, S.; Ochterski, J.; Petersson, G. A.; Ayala, P. Y.; Cui, Q.; Morokuma, K.; Malick, D. K.; Rabuck, A. D.; Raghavachari, K.; Foresman, J. B.; Cioslowski, J.; Ortiz, J. V.; Stefanov, B. B.; Liu, G.; Liashenko, A.; Piskorz, P.; Komaromi, I.; Gomperts, R.; Martin, R. L.; Fox, D. J.; Keith, T.; Al-Laham, M. A.; Peng, C. Y.; Nanayakkara, A.; Gonzalez, C.; Challacombe, M.; Gill, P. M. W.; Johnson, B. G.; Chen, W.; Wong, M. W.; Andres, J. L.; Head-Gordon, M.; Replogle, E. S.; Pople, J. A. *Gaussian 98*, revision A.7; Gaussian, Inc.: Pittsburgh, PA, 1998. (b) Frisch, M. J.; Trucks, G. W.; Schlegel, H. B.; Scuseria, G. E.; Robb, M. A.; Cheeseman, J. R.; Montgomery, J. A., Jr.; Vreven, T.; Kudin, K. N.; Burant, J. C.; Millam, J. M.; Iyengar, S. S.; Tomasi, J.; Barone, V.; Mennucci, B.; Cossi, M.; Scalmani, G.; Rega, N.; Petersson, G. A.; Nakatsuji, H.; Hada, M.; Ehara, M.; Toyota, K.; Fukuda, R.; Hasegawa, J.; Ishida, M.; Nakajima, T.; Honda, Y.; Kitao, O.; Nakai, H.; Klene, M.; Li, X.; Knox, J. E.; Hratchian, H. P.; Cross, J. B.; Bakken, V.; Adamo, C.; Jaramillo, J.; Gomperts, R.; Stratmann, R. E.; Yazyev, O.; Austin, A. J.; Cammi, R.; Pomelli, C.; Ochterski, J. W.; Ayala, P. Y.; Morokuma, K.; Voth, G. A.; Salvador, P.; Dannenberg, J. J.; Zakrzewski, V. G.; Dapprich, S.; Daniels, A. D.; Strain, M. C.; Farkas, O.; Malick, D. K.; Rabuck, A. D.; Raghavachari, K.; Foresman, J. B.; Ortiz, J. V.; Cui, Q.; Baboul, A. G.; Clifford, S.; Cioslowski, J.; Stefanov, B. B.; Liu, G.; Liashenko, A.; Piskorz, P.; Komaromi, I.; Martin, R. L.; Fox, D. J.; Keith, T.; Al-Laham, M. A.; Peng, C. Y.; Nanayakkara, A.; Challacombe, M.; Gill, P. M. W.; Johnson, B.; Chen, W.; Wong, M. W.; Gonzalez, C.; Pople, J. A. *Gaussian 03*, revision C.02; Gaussian, Inc.: Wallingford, CT, 2004.
- (29) (a) Cromwell, N. H.; Hoeksma, H. *J. Am. Chem. Soc.* **1945**, *67*, 1658. (b) Lee, H.; Kitagawa, T. *Bull. Chem. Soc. Jpn.* **1986**, *59*, 2897.
- (30) Grabowska, A.; Kownacki, K.; Kazmarek, L. *Acta Phys. Pol. A* **1995**, *88*, 1081.
- (31) Fabian, W. M. F.; Antonov, L.; Nedeltcheva, D.; Kamounah, F. S.; Taylor, P. J. *J. Phys. Chem. A* **2004**, *108*, 7603.
- (32) (a) Destro, R.; Gavezzotti, A.; Simonetta, M. *Acta Crystallogr. B* **1978**, *34*, 2867. (b) Arod, F.; Gardon, M.; Pattison, P.; Chapuisa, G. *Acta Crystallogr. C* **2005**, *61*, o317.
- (33) Champagne, B.; Perpète, E. A.; Jacquemin, D.; van Gisbergen, S. J. A.; Baerends, E. J.; Soubra-Ghaoui, C.; Robins, K. A.; Kirtman, B. *J. Phys. Chem. A* **2000**, *104*, 4755.
- (34) (a) Champagne, B.; Bishop, D. M. *Adv. Chem. Phys.* **2003**, *41*, 126. (b) Guillaume, M.; Botek, E.; Champagne, B.; Castet, F.; Ducasse, L. *J. Chem. Phys.* **2004**, *121*, 7390.